GEOTECHNICAL AND GEOPHYSICAL CHARACTERIZATION OF SULMONA BASIN LACUSTRINE SILTS AND CLAYS FOR SEISMIC MICROZONATION PURPOSES

Ciaglia S., Pagliaroli A.°, Pizzi A., Francescone M., Amoroso S.*, Salvatore N.
Dipartimento di Ingegneria e Geologia (INGEO), Università di Chieti-Pescara
** Istituto Nazionale di Geofisica e Vulcanologia, L'Aquila*
° e-mail (corresponding): alessandro.pagliaroli@unich.it

Ashayeri I.
Civil Eng. Dept., Razi University, Kermanshah, Iran

Abstract

The paper deals with the mechanical properties of lacustrine silts and clays filling most of the Sulmona basin. The characterization of these sediments to a depth higher than 500 m is a crucial step for the Seismic Microzonation of the area and it has been addressed by a multidisciplinary approach including geological analysis, active and passive geophysical investigations, geotechnical laboratory testing, numerical modelling, processing of available strong motion recordings.

1. Introduction

The city of Sulmona (Central Italy) lies above a deep sediment-filled intermontane basin (Sulmona basin) characterized by complex geological, geomorphological, and tectonic setting. Relevant site effects related to impedance contrast between the fine-grained lacustrine sediments, which represent the main filling of the basin and the underlying carbonate bedrock and to buried morphological/tectonic features, are expected. The unfavorable local conditions coupled with the presence of Mt. Morrone active and capable normal fault bordering the NE sector for the basin, determine high seismic hazard level for the city of Sulmona and neighboring villages. The present paper focuses on the geotechnical characterization of lacustrine soils, drilled and sampled for hundreds of meters deep controlling the seismic response of the area. The Vs-profile and the cyclic nonlinear properties in the lacustrine sediments for third level Seismic Microzonation (SM) study are inferred.

2. Geological and seismological setting

The Sulmona basin is an intermontane depression elongated for 20 km in the NW-SE direction and up to 5-7 km wide. The tectonic origin of the basin is due to the Quaternary activity of the Mt. Morrone normal fault which dips to the south-west limiting the NE edge of the basin (Miccadei et al. 1998), capable of surface coseismic rupture and potentially able to produce M 6.5–6.7 earthquakes. The basin infill of such an half-graben shows a typical triangular geometry thickening toward the Mt. Morrone boundary fault plane, where the Pliocene?-Quaternary lacustrine-fluvial sequence should reach up to 500-600 m of thickness (Miccadei et al., 1998) although the entire sequence has never been observed in either an outcrop or in a borehole. Water wells data that have reached depths of a few hundred meters, however, show that most of the filling deposit consist of fine-grained lacustrine silts and clays, to which levels and lenses of fluvial-alluvial gravelly sands, up to few tens of meters thick, are interstratified. A gravelly sand deposition also characterizes the Late Quaternary alluvial plains that first overlayed the top of the lacustrine sequence and then were carved into as fluvial terrace deposits

(Salvatore et al., 2022).

3. Characterization of lacustrine silts and clays

3.1 Representative cross-section and available data

The location of available boreholes, in-hole tests, noise measurements and seismic arrays are reported in the simplified geological map of Figure 1. Data collected from previous studies have been integrated with investigations planned in the framework of third level SM project including a 200 m deep borehole (SR in Figure 1). The locations of the four permanent strong motion stations of the Italian Accelerometric Network (RAN) are also reported. Stations SULA and SULC are installed in the center of the basin, SULP in correspondence of a debris alluvial fan while SUL is installed at rock outcrop. The depth reached by deep boreholes, which never intercepted the carbonate bedrock, is shown. A representative cross-section NN' has been selected to study the seismic response of the basin whose trace is almost coincident with the RAN stations alignment. Available data allowed to define a preliminary subsoil model for NN' cross-section aimed at site response analysis (Figure 2). Carbonate bedrock (unit 9) outcrops at the border of the basin while the inner part shows a depocenter deep more than 500 m and filled by a thick fine lacustrine succession on which lay a sandy-gravel terraced alluvial deposits (units 1 and 2, 30-40 m thick). A continuous coarse layer (unit 4), intercepted by boreholes, has been identified in the fine-grained lacustrine succession (units 3 and 5). A mainly coarse alluvial-lacustrine layer (unit 6) can be identified at SW edge. Major uncertainty does exist at the NE edge of the basin: unit 8 characterized by lower stiffness than unit 9 has been introduced to define the strongly cataclasic bedrock passing laterally to the slope deposits-alluvial fan (unit 7).

3.2 Laboratory data

Nine undisturbed samples of lacustrine silts were recovered in SR deep borehole (Figura 1) and seven subjected to identification and classification tests as well as to static and cyclic tests. Depth of the samples and corresponding tests carried out are presented in Table 1 together with main physical and mechanical properties. The material is a clayey silt with sand content generally lower than 10%. According to the Casagrande classification chart, the soil is essentially an inorganic clay of medium plasticity (average PI = 18). The material is slightly overconsolidated with OCR around 3 in the upper part of the deposit. Cyclic nonlinear properties were measured with the Double Specimen Direct Simple Shear (DSDSS) device, developed at the University of Rome "La Sapienza" (Lanzo et al., 2009). Cyclic tests were carried out on three samples at the estimated in situ vertical effective stress and higher confining pressures to simulate higher depths. Overall, nine confining pressure were applied in the tests with σ'_v ranging from 200 to 1700 kPa which is the highest value applicable in the device. Experimental data define a very narrow area for both normalized shear stiffness (G/G_0) and damping ratio (D) curves thus indicating a moderate influence of the confining pressure on the nonlinear behavior. This behavior is also confirmed by resonant column tests performed on lacustrine deposits in the historical center of Sulmona (Madiai et al., 2022). The ranges of nonlinear curves are reported in Figure 3 and compared with the curves proposed by Ciancimino et al. (2020) based on a large database of fine-grained Italian soils. Moreover, the measurement of small-strain shear modulus G_0 at different confining pressures allowed to define the variation of stiffness with the mean effective stress p': $G_0 = 0.62 \cdot (p')^{0.81}$ with G_0 expressed in MPa and p' in kPa. The function can be converted as $V_S = 56 \cdot z^{0.334}$ with the depth z from ground level expressed in m. Laboratory tests allow to define the stiffness gradient with depth while absolute values of G_0/V_S are obviously underestimated with respect to in situ stiffness mainly due to sample disturbance.

Table 1. Laboratory test carried out on lacustrine silts samples recovered from SR borehole and main physical and mechanical properties. LEGEND: ID: identification/classification tests, ED: oedometer test; TD: direct shear test; DSDSS: double specimen direct simple shear cyclic test; Gr-Sa-Si-Cl: soil types from grain size distribution; W_L: liquid limit; W_P: plasticity limit; PI: plasticity index; γ: unit weight; OCR: overconsolidation ratio; Cc: compression index; c' and φ': effective cohesion and friction angle.

Sample	**Depth**	**test**	**Gr-Sa-Si-Cl**	**W_L**	**W_P**	**PI**	**w**	**γ**	**OCR**	**Cc**	**c'**	**φ'**
	(m)	-	(%)	(%)			(%)	(kN/m^3)	(-)	(-)	(kPa)	(°)
CI2	23.6	ID,ED,DSDSS	1-11-69-19	38	23	15	30	18.8	3.1	0.28	-	-
CI3	40.3	ID,ED,DSDSS	0-3-83-14	52	27	25	45	16.6	2.2	0.50	-	-
CI4	78.3	ID,TD	0-11-66-23	46	24	22	34	18.2	-	-	60	23
CI5	124.3	ID,ED,DSDSS	1-8-70-21	45	26	19	31	18.2	1.6	0.45	-	-
CI6	135.3	ID,ED	0-6-73-21	45	27	18	38	17.9	-	0.32	-	-
CI8	159.3	ID,TD	0-3-69-28	37	20	17	24	19.6	-	-	113	23
CI9	186.3	ID,ED	0-2-72-26	43	30	13	35	18.0	np	np	-	-

3.3 Geophysical data

A total number of 14 down-hole and cross-hole tests executed in the basin and intercepting lacustrine silts were recovered. Additional down hole (DH) tests, planned for third level SM, are in progress. The V_S profiles measured in the five DH tests carried out close to NN' cross-section (around 2 km from the trace) are plotted in Figure 4. Meanwhile, the strong-motion records at SULC were investigated for the calculation of earthquake horizontal to vertical spectral ratio (eHVSR). Figure 5 presents the observed eHVSR from 18 events recorded at SULC with $4.1 < Mw < 6.5$ and $1 < PGA < 50$ cm/s^2. The eHVSR was used for the retrieval of V_S profile based on the diffuse field concept of Kawase et al. (2011) and by a recent optimization algorithm of Ashayeri et al. (2022). The inversion best misfit eHVSR curve is compared with the observed eHVSR curve in Figure 5, and its corresponding V_S profile is shown in Figure 4. The inversion algorithm presents the V_S profile down to depth of about 4.6 km corresponding to seismic bedrock, but only the shallower 500 m is presented here.

3.4 Back-analysis of resonance frequencies across the basin

An extensive noise measurements survey was carried out in the basin. The location of measurements with the indication of the fundamental resonance frequency f_0 derived from HVSR technique is shown in Figure 1. The experimental values of f_0 along the NN' cross-section allowed a validation of the subsoil model in the linear range. Assuming the geometry in Figure 2 and the geotechnical properties in Table 2 a comparison between experimental f_0 and the numerical values computed from 2D numerical linear visco-elastic amplification functions has been undertaken. Note that the V_S values assumed for the different units are based on the available geophysical tests, in particular for the gravelly layer (unit #4) and the lacustrine silts (unit 3 and 5) the results of passive array close to SULA (figure 1) were used. The analyses were carried out with the 2D finite element code LSR2D (www.stacec.com). The amplification functions present multiple peaks due to the complex physical phenomena affecting the seismic response of the basin; the first 3 natural frequencies (f_1-f_2-f_3) have been compared with the experimental f_0. At the center of the basin a good agreement between experimental frequencies and the first numerical frequency ($f_1 \cong 0.4$Hz) is observed (Figure 6); further considerations not reported here suggest the possible occurrence of 2D resonance of the valley at frequency f_1. At the edges of basin, complex 2D effects take place and the experimental f_0 is well matched by higher order natural frequencies (f_2 or f_3, Figure 6). Overall, the good agreement between numerical and experimental natural frequencies suggests a reliable geometrical-mechanical model assumed for the basin, including the V_S profile for the lacustrine silts.

Table 2. Subsoil model assumed for 2D linear visco-elastic site response analyses (see cross-section in Figure 2); damping ratio D was assumed as 2% for units 1-2, 0.5% for bedrock, 1% for all the remaining units

Unit	Description	γ	Vs	ν	Unit	Description	γ	Vs	ν
		(kN/m^3)	(m/s)	(-)			(kN/m^3)	(m/s)	(-)
#1	Sandy gravels	20	200	0.35	#6	Alluvial-lacustrine dep.	21	600	0.48
#2	Gravels	21	500	0.35	#7	Alluvial fan/slope dep.	22	1400	0.35
#3	Lacustrine silts	17.9	400	0.47	#8	Jointed bedrock	22	1800	0.30
#4	Gravels/sands	22	1000	0.44	#9	bedrock	23	2500	0.30
#5	Lacustrine silts	18.4	800	0.47					

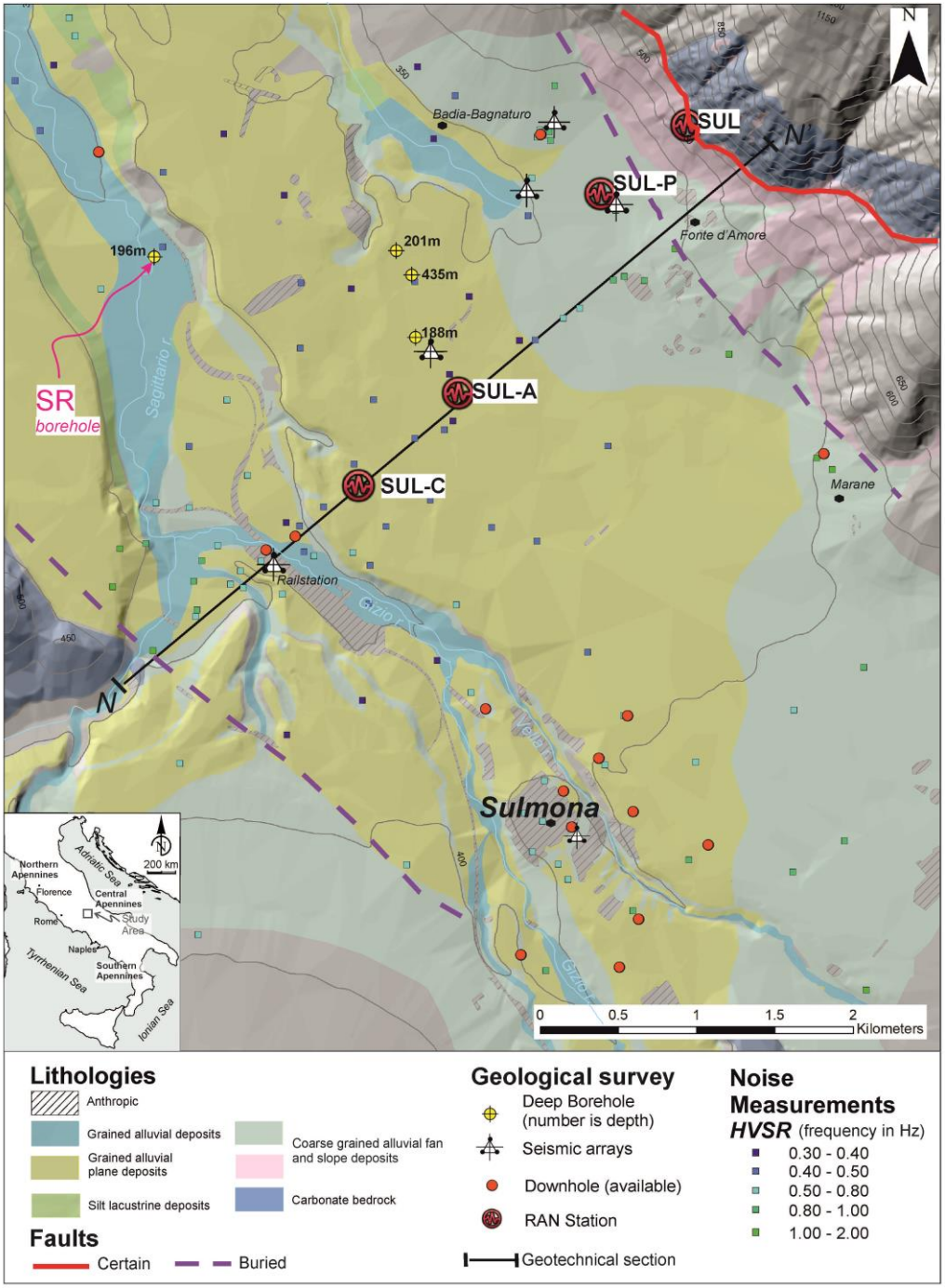

Fig 1. Simplified geological map of the Sulmona basin with the location of boreholes, geophysical investigations, permanent strong motion stations (RAN network); trace of the representative NN' cross-section is also shown

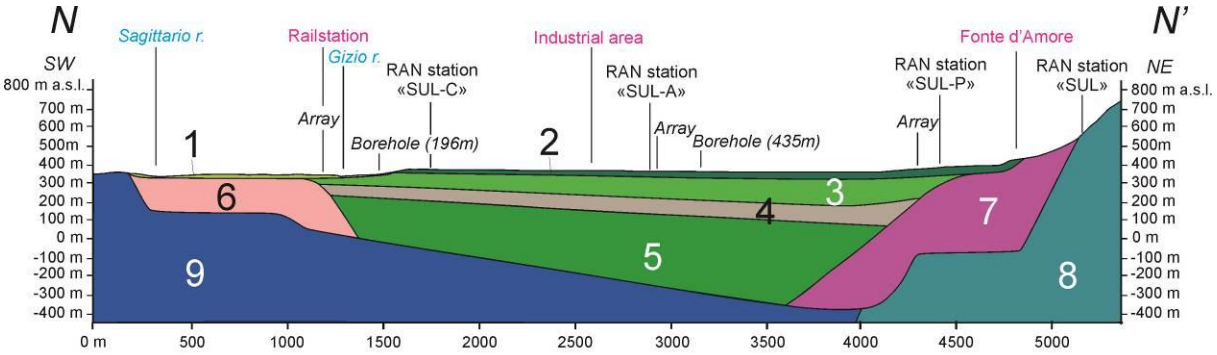

Fig 2. Subsoil model for NN' cross-section of the Sulmona basin; see table 2 for the geotechnical characterization of units 1-9

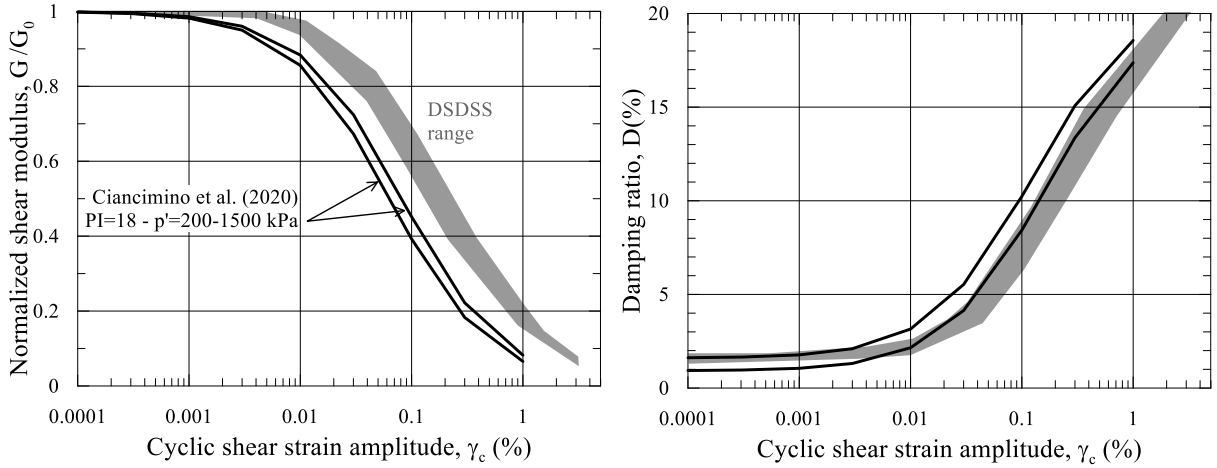

Fig 3. Normalized shear modulus and damping ratio curves for lacustrine silts from cyclic tests and comparison with literature data

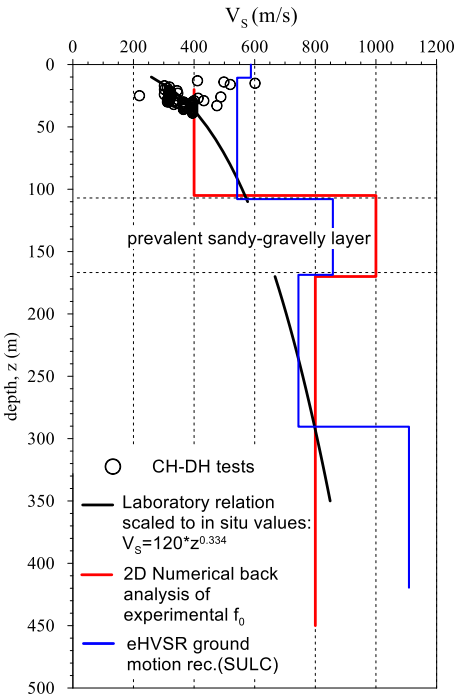

Fig 4. Vs profile in the lacustrine clays according to different approaches

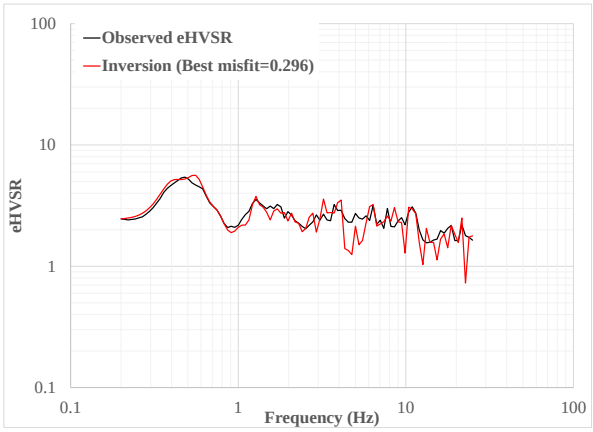

Fig. 5. eHVSR of the observed strong motions and inversion (Best misfit) at SULC

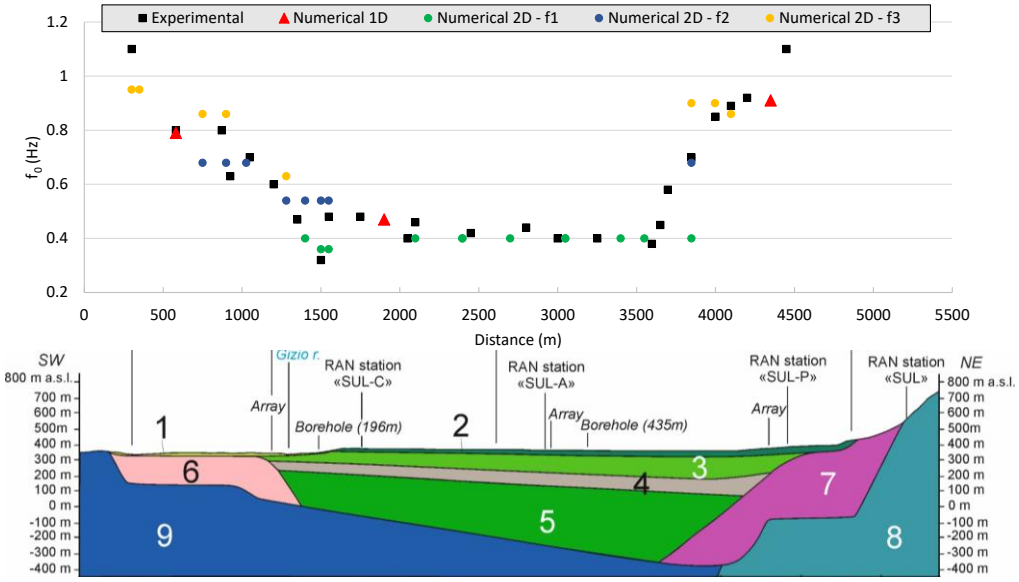

Fig 6. Experimental and numerical resonance frequencies across the basin

4. Discussion, conclusions, and open issues

The seismic response of Sulmona basin is mainly controlled by complex buried morphological features and the mechanical properties of lacustrine soils filling most of the valley. The characterization of these sediments to a depth higher than 500 m is a challenging task and it has been addressed in this paper by a multidisciplinary approach. A stiffness-depth relation derived from cyclic laboratory tests and calibrated on in-hole tests has been integrated with V_S profiles from inversion of recordings from a ground motion station (eHVSR) and from a 2D numerical back-analysis of resonance frequencies from single-station noise measurements. The V_S profile has been constrained for the whole thickness of lacustrine silts even if some uncertainties exist in the upper portion and close to the bedrock where eHVSR provide higher stiffness. In progress inversion at SULA will provide additional data and further 2D numerical analyses using rock recorded motion SUL as input and SULA/SULC recordings as target output will be executed. Regarding nonlinear cyclic properties of lacustrine soils, a more linear and less dissipative behavior with respect to clays of similar plasticity has been observed; the role of possible organic content and cementations bonds will be investigated.

Bibliografia

Ashayeri, I., Nagashima, F., Kawase, H., Dashti, M.T. (2022). "Application of a Telescopic Evolutionary Algorithm with the Diffuse-Field Concept for Velocity Inversion from Strong Motion Data at K-NET and KiK-net Stations in the Presence of Borehole and Geological Data", *Soil Dynamics & Earth. Eng.*, under revision.

Ciancimino A., Lanzo G., Alleanza G.A., Amoroso S., Bardotti R. et al. (2020). "Dynamic characterization of fine-grained soils in Central Italy by laboratory testing", *Bulletin of Earthquake Engineering*, 18:5503-5531.

Kawase, H., Sánchez-Sesma, F.J., Matsushima S. (2011). "The Optimal Use of Horizontal-to-Vertical Spectral Ratios of Earthquake Motions for Velocity Inversions Based on Diffuse-Field Theory for Plane Waves", *Bulletin of the Seismological Society of America*; 101(5), 2001–2014. doi: https://doi.org/10.1785/0120100263.

Lanzo G., Pagliaroli A., Tommasi P., Chiocci F. L. (2009). "Simple shear testing of sensitive, very soft offshore clay for wide strain range", *Canadian Geotechnical Journal*, 46(11), 1277-1288.

Madiai C., Ciardi G., Manuel M., Galadini F., Amoroso S. (2022). "Site characterization and preliminary ground response analysis for the monumental Complex of SS. Annunziata in Sulmona, Italy", Proc. Geotechnical Engineering for the Preservation of Monuments and Historic Sites III, Naples 2022: 800-811.

Miccadei E., Barberi R. & Cavinato G.P. (1998). "La geologia quaternaria della conca di Sulmona (Abruzzo, Italia centrale)", *Geologica Romana*, 34, 59-86. [In Italian].

Salvatore N., Pizzi A., Rollins K., Pagliaroli A., Amoroso S. (2022). "Liquefaction assessment of gravelly soils: the role of in situ and laboratory geotechnical tests through the case study of the Sulmona basin (Central Italy)", *Ital. J. Geosci.*, 141(2), 216-229.